Proceedings of the Project Review, Geo-Mathematical Imaging Group (Purdue University, West Lafayette IN), Vol. 1 (2010) pp. 211-220.

SEISMIC WAVE PROPAGATION IN FRACTURED CARBONATE ROCK

WEIWEI LI* AND LAURA J. PYRAK-NOLTE†

Abstract. Laboratory experiments were performed on cubic samples of Austin Chalk to investigate the effect of fabric-induced anisotropy on the interpretation of fracture specific stiffness. The experimental results found that the fabric-induced layering complicates the interpretation of fracture specific stiffness. Seismic measurements from a sample with small layers (i.e., spacing and thickness) show that the presence of the fracture tends to interrupt the interference caused by short-path multiples and also tends to increase the high frequency components of the signal. This increase in the high frequency components is inconsistent with the prediction from the displacement discontinuity theory. For a fractured sample with only three distinct layers (i.e., large spacing and thickness), the high frequency components of the seismic waves were attenuated as expected by the displacement discontinuity theory. To investigate how the presence of a single fracture in a periodically layered medium affects seismic waves, numerical simulations were performed by combining a transfer matrix method with the displacement discontinuity theory for wave propagation across a fracture. From our current simulation results for a normally incident wave, in general, a fracture in a layered media behaved as a low pass filter and did not reproduce the behavior observed in the sample with thin layers. Future work will examine incident angles and fracture orientations that more closely match those from the experiments.

1. Introduction. Layering, fractures and other mechanical heterogeneities are common to most rock and often are sources of mechanical and hydraulic anisotropy. In periodically layered medium, multiple reflections in thin layers arrive immediately following the primary signal. In addition, these multiple reflections from many thin layers can interfere constructively resulting in a wave component with an amplitude comparable to the primary wave (O.Doherty and Anstey 1971). Waves propagating in periodically layered medium have been well studied using a variety of theoretical techniques (e.g., Aki & Richards, 1980; Crampin, 1981; Mal 1988; Petrashen, 2003). Exact solution for wave propagation in a layered medium can be acquired by adapting transfer matrix method. In this paper, we combine the transfer matrix method with the displacement discontinuity theory for wave propagation across a single fracture. Several investigators have used the displacement discontinuity boundary conditions to analyze wave propagation through fractures. The general solution for compressional and shear waves propagated at oblique angles of incidence to a displacement discontinuity is given by Schoenberg [1980] and Kitsunezaki [1983]. Myer et al. [1985] showed that the displacement discontinuity model predicted correctly the amplitude behavior of waves propagated across synthetic fractures of calculable stiffness. Pyrak-Nolte et al. [1990a] showed that the effect of a single natural fracture on spectral amplitudes for transmission of compressional and shear pulse is described well by the displacement discontinuity model. However, as described in this paper, we have observed that layering in Austin Chalk makes it difficult to interpret fracture stiffness from experiment results. Therefore numerical simulations were undertaken to study the combined effect of anisotropy from layering and a single fracture on seismic attenuation and the spectral content of the signal.

2. Experimental Method. Experiments were performed on Austin Chalk Cordova Cream samples (labeled as AC1 and AC7) obtained from Texas Quarries. Fractured samples (AC1 FRAC and AC7 FRAC) were created by inducing a single fracture approximately perpendicular to the layers in an intact sample of Austin Chalk (edge length 100 mm) using a technique similar to brazil testing (Jaeger & Cook, 1979).

The fabric-induced layering differed between the two samples used in this study as shown in Figure 1. AC1 contained interleaved brown and white layers while AC7 has several clear brown layers. The layers in AC7 were thicker than the layers in AC1. The visual observations about the structure of the samples was confirmed from X-ray tomographic scans (Figure 2) on companions samples to AC1 (ACS3 companion) and AC7 (AC4LW companion). In the CT results, clear layering

*Department of Physics, Purdue University, West Lafayette, IN 47907

†Department of Physics, Purdue University, West Lafayette, IN 47907, Department of Earth and Atmospheric Sciences, Purdue University, West Lafayette, IN 47907

TABLE 2.1
Density and Velocities of the sample.

	Density (kg/m^3)	P velocity (m/s)	S velocity (m/s)
AC1	2052	3427	2088
AC7	1991	3448	2041

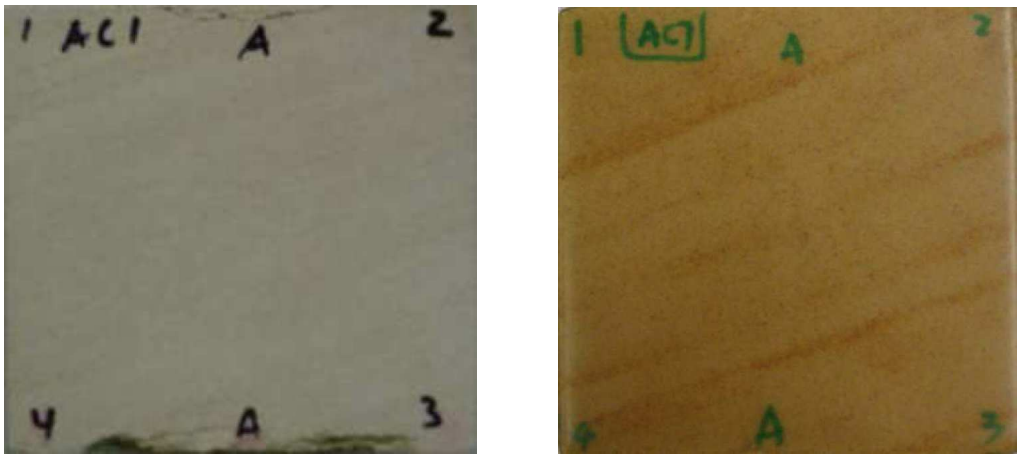

FIG. 1. *Images of samples AC1 (left) and AC7 (right)*

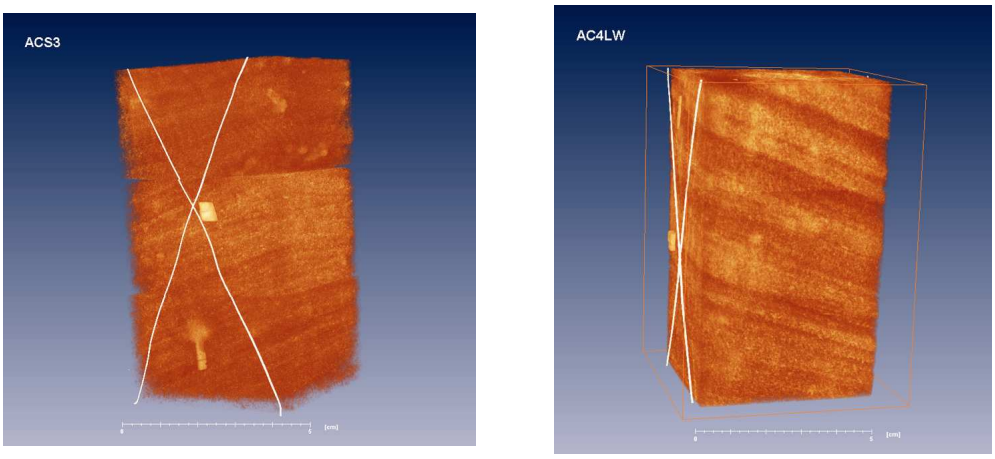

FIG. 2. *CT scan of sample ACS3 (left) and AC4LW (right)*

is observed in the companion sample to AC7 (AC4LW), while the CT scan from the companion sample to AC1 shows many very fine layers and appears to be homogeneous.

A seismic array was used to perform full-waveform measurements on the samples and is shown in Figure 3. Compressional and shear wave contact piezoelectric transducers (each with a central frequency of 1.0MHz) were used. The transducer layouts for the source and receiver plates were mirror images of each other. For this study, signals transmitted from source Plate B to receiver Plate B were used. The orientation of the layers and fracture in the Austin Chalk sample are also shown in Figure 3.

3. Simulation.

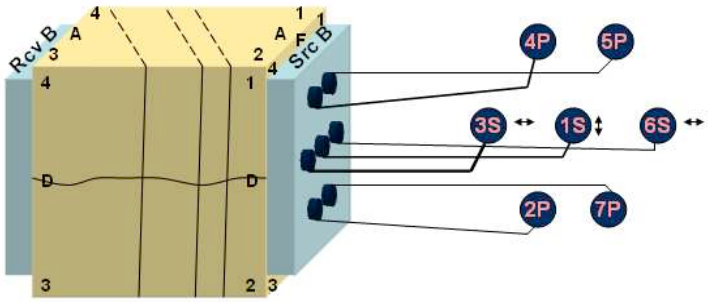

FIG. 3. *Seismic Array Setup, Experiment Setup showing the transducer configuration. P represents compressional wave transducers. S represents shear wave transducers. The arrow shows the polarization of shear wave transducer. Solid lines and dash lines represent the layers in the rock. The curve line on face D of the sample represents the fracture.*

3.1. Displacement Discontinuity Theory. In the displacement discontinuity theory, a fracture is modeled theoretically as a non-welded contact and it is assumed that the fracture has a negligible thickness compared to the seismic wavelength. A non-welded contact is represented by a set of boundary conditions between two elastic half spaces. The boundary conditions that describe a non-welded contact are (1) stress across the fracture is continuous ($\sigma_1 = \sigma_2$), but (2) the displacement is not. The magnitude of the discontinuity in displacement is inversely proportional to the specific stiffness of the fracture ($u_2 - u_1 = \sigma/k$). Subscripts 1 and 2 refer to upper and lower elastic media. The displacement discontinuity theory results in frequency dependent transmission and reflection coefficients for a purely elastic model.

The solution matrix for a SH wave propagated across a fracture (or non-welded contact) is:

$$\begin{bmatrix} -\kappa & \kappa - \mathrm{i}\omega\rho_2\beta_2\cos j_2 \\ \rho_1\beta_1\cos j_1 & \rho_2\beta_2\cos j_2 \end{bmatrix} \begin{bmatrix} r_f \\ t_f \end{bmatrix} = \begin{bmatrix} \kappa \\ \rho_1\beta_1\cos j_1 \end{bmatrix}$$

where κ, ρ, β, and j are fracture specific stiffness, density, shear wave velocity and incident angle separately.

In our simulations, we assume the upper and lower media are the same and have the same transmission and reflection coefficients:

$$t_f = \frac{B}{B - \mathrm{i}\cos j}, \qquad r_f = -\frac{\mathrm{i}\cos j}{B - \mathrm{i}\cos j}$$

where $B = 2\kappa/\omega\rho\beta$.

From this formulation, a fracture behaves as a low pass filter. Transmission decreases as frequency increases and increases as the incident angle increases (Figure 4).

3.2. Transfer Matrix Method. A transfer matrix approach was used to simulate wave propagation in a layered medium. First, we define one layer that includes Medium 2 and the welded interface between Medium 1 and Medium 2 (see Figure 5). For the one layer system shown in Figure 5, the transfer matrix M is:

$$\begin{bmatrix} U_1 \\ D_1 \end{bmatrix} = \frac{1}{t_{12}} \begin{bmatrix} 1 & t_{21} \\ r_{12} & 1 \end{bmatrix} \begin{bmatrix} 1/\sqrt{Z} & 0 \\ 0 & \sqrt{Z} \end{bmatrix} \begin{bmatrix} U_2 \\ D_2 \end{bmatrix}$$

$$M = \frac{1}{t_{12}} \begin{bmatrix} 1 & t_{21} \\ r_{12} & 1 \end{bmatrix} \begin{bmatrix} 1/\sqrt{Z} & 0 \\ 0 & \sqrt{Z} \end{bmatrix}$$

where t, r, are the transmission and reflection coefficients for the welded interface, $Z = e^{\mathrm{i}\omega T}$, and T is the two way travel time, $T = h\cos j/\beta$. Thus, the exact solution for a periodically layered medium with one parallel fracture can be calculated with the following equation:

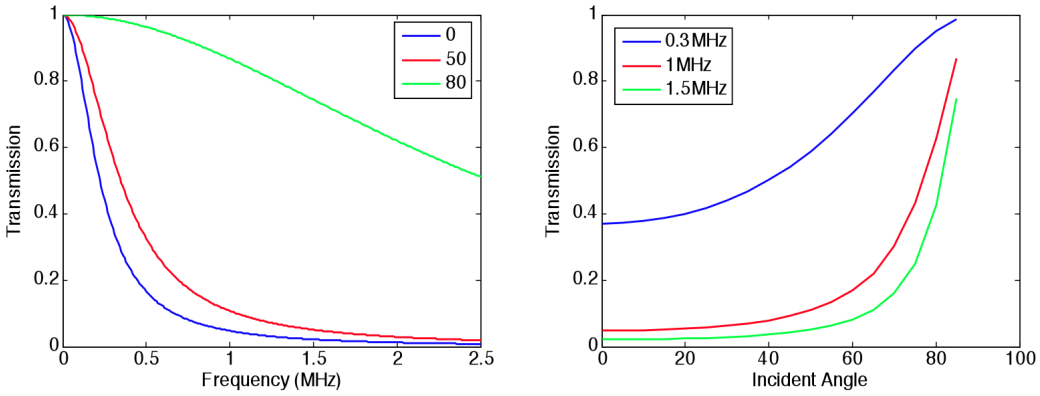

FIG. 4. *(left) Transmission as a function of frequency for three different incident angles, 0°, 50° and 80°. (right) Transmission as a function of incident angle for three different frequencies (0.3 MHz, 1 MHz, 1.5 MHz).*

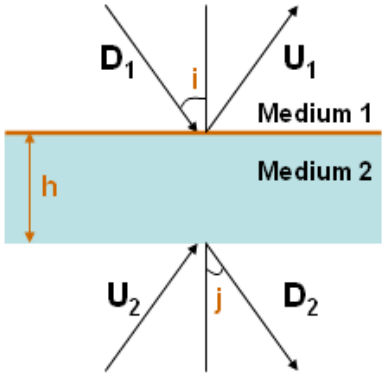

FIG. 5. *Waves incident, reflected and transmitted through one layer.*

$$\begin{bmatrix} U_1 \\ D_1 \end{bmatrix} = M_1 M_2 \cdots M_f \cdots M_k \frac{1}{t_{kk+1}} \begin{bmatrix} 1 & t_{k+1k} \\ r_{kk+1} & 1 \end{bmatrix} = M \begin{bmatrix} U_{k+1} \\ D_{k+2} \end{bmatrix}$$

where,

$$M_f = \frac{1}{t_f} \begin{bmatrix} 1/\sqrt{Z} & -r_f\sqrt{Z} \\ r_f/\sqrt{Z} & (t_f^2 - r_f^2)\sqrt{Z} \end{bmatrix}$$

is the transfer matrix for a fractured layer.

4. Results and Discussion.

4.1. Experimental results. Wavelet analyses were applied to waves recorded using source-receiver pairs 2P-4P for the intact and fractured samples AC1 and AC7. The transmitted compressional signals, the spectra of these signals and the wavelet transforms of these signals are shown in Figure 6 and Figure 7 for samples AC1 and AC7, respectively. For intact sample AC1, two waves are observed to arrive closely together with comparable amplitudes and these waves produce a long period first arrival wave package (black line in Figure 6a). This wave interference results in a dominant frequency of roughly 0.3MHz. After a fracture was induced in sample AC1, the interference was interrupted and the dominant frequency of the first arrival increased to $\sim$ 0.4MHz. The increase in the dominant frequency component after fracturing was not observed in sample AC7. Apparently, waves through either intact or fractured AC7 exhibit wave packages that contain

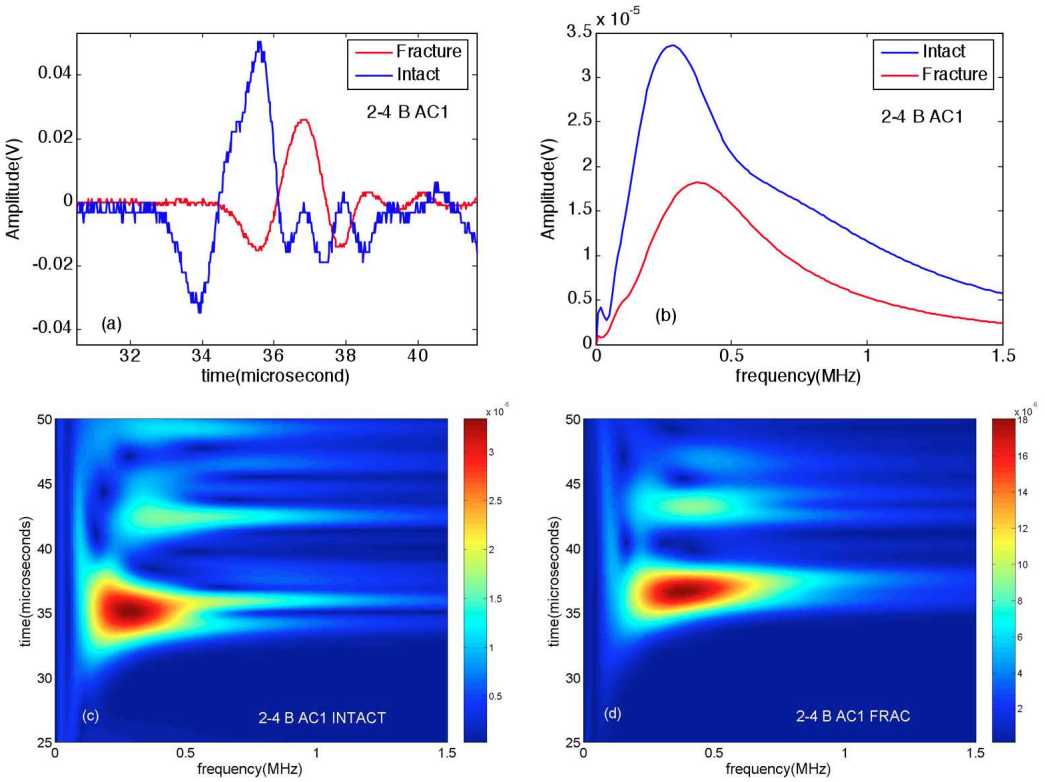

FIG. 6. *Waveforms, spectra and wavelet from the intact and fracture AC1.*

waves that arrive very closely and interfere. For fractured sample AC7, the presence of a fracture generated even more internal reflections that arrived following the first arrival as can be seen in the wavelet transform (Figure 7d).

From visual inspection and X-ray tomographic scans, the layer thickness and layer properties varied among samples of Austin Chalk from the Cordova Crme formation. Li et al. (2009) showed from thin sections and X-ray tomographic scans that Austin chalk, though being made up 99% of calcite, varied in density. Considering the different layering in these two samples, the question arises: what effect will a fracture have on waves propagating through a finely layered medium with interleaved high and low impedance layers? This is the motivation for using both the transfer matrix method and the displacement discontinuity theory for simulating fractured periodically layered media.

4.2. Simulation Results. Consider a plane shear wave propagated through a layered cell of stacked Medium 1 and Medium 2 (Figure 5). The density and shear wave velocity of Medium 1 are 1800 kg/m^3 and 3000m/s, respectively. While the density and shear wave velocity of Medium 2 are 2000 kg/m^3 and 3400m/s, respectively. Medium 1 has a thickness of 0.75 mm and Medium 2 has a thickness of 2.25 mm. Medium 1 and Medium 2 compose the layered cell. Simulations were performed with 1, 3, 5, 10 and 20 layered cells. A fracture was located in the middle of the middle layered cell in Medium 2. The input or source signal was a transmitted compressional wave from an aluminum standard with the same dimensions as the samples in the experiments. The signal from the aluminum sample had a Gaussian spectrum from 0 to 2MHz with a maximum or dominant frequency of 1MHz. In the simulations, the incident angle was varied between 0° to 85° in increments of 5°. A wavelet analysis was used to extract the spectrum of simulated seismic wave.

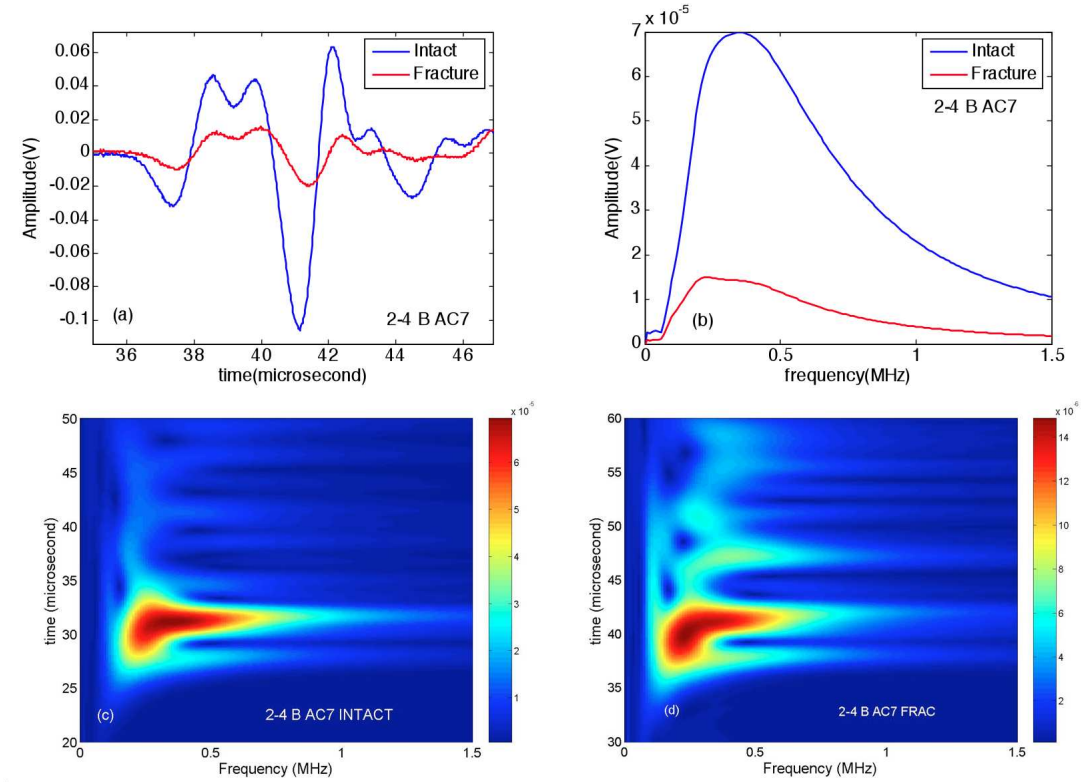

FIG. 7. *Waveforms, spectra and wavelet from the intact and fracture AC7.*

4.2.1. Effect of number of layered cells. An analysis was performed for simulated samples that contained a single fracture and either 1, 3, 5, 10, or 20 layered cells. In Figure 8, we compare the relative transmission as a function of frequency for different number of layered cells. The relative transmission is defined as the ratio of the spectral amplitude for wave transmission through a fractured layered medium to that from the same layered medium without a fracture. The simulation results indicate that the relative transmission caused by the fracture (with fracture specific stiffness of $5x10^{12}$ Pa/m) is independent of the number of layered cells and that the functional form of the relative transmission versus frequency closely mimics that of transmission across a single fracture in an non-layered medium (Figure 8a). The ratio of the dominant frequency (from the layered-fractured case to that of the layered case) found that the dominant frequency ratio increases as number of layered cells increased (Figure 8b). The occurrence of multiple reflections caused by the layers is observed in the wavelet transforms shown in Figure 9. As the number of layered cells increased from 5 to 20, the amplitude of second arrival increased because of the increase in multiples. However, the presence of a fracture did not weaken the interference but tended to produce additional multiples that arrive later. This is similar to the behavior observed for sample AC7.

4.2.2. Effect of incident angle. We have also examined the effect of angle of incidence on the time-frequency behavior for waves propagated through a fractured layered medium. In this section, we present simulation results as a function of angle of incidence (0° to 85°). Relative transmission as a function of incident angle was found to be independent of the number of layers (Figure 10a) and increased as the incident angle increased. From Figure 10b, the ratio of the dominant frequency decreased for incident angles up to 45° and then increased for angles greater than 45° independent of the number of layered cells. The incident angle does have an effect on the dominant frequency.

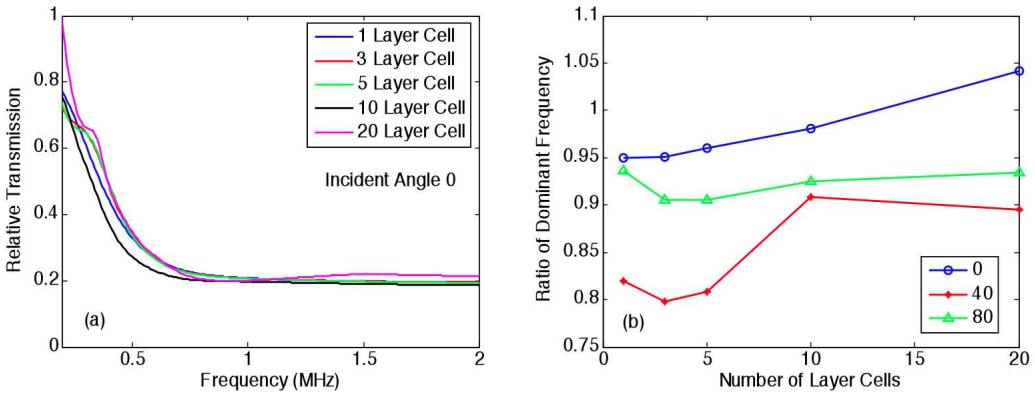

FIG. 8. *(left) Normalized attenuation as a function of Frequency with different number of layer cells; (right) Dominant Frequency as a function of number of layer cells with different incident angles.*

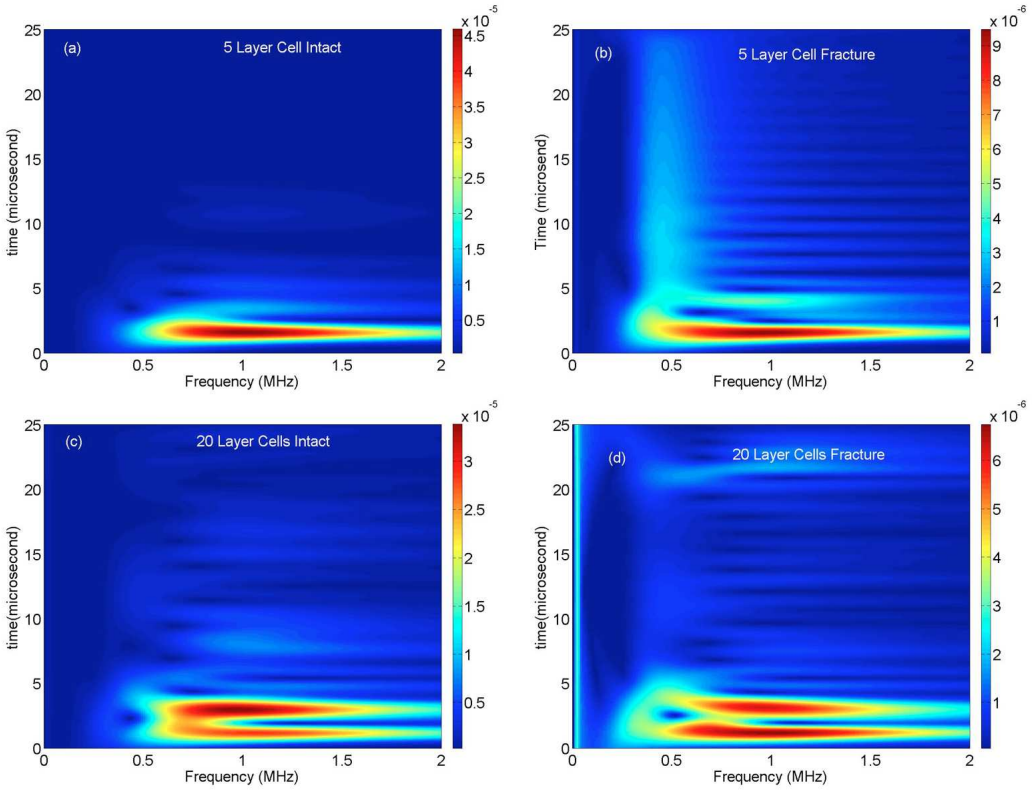

FIG. 9. *(a) & (b) Wavelet transform for an intact and fractured media with 5 layered cells at normal incidence. (c) & (d) Wavelet transform for intact and fractured media with 20 layer cells at normal incidence.*

The minimum dominant frequency ratio indicates roughly a 20% change in the dominant frequency caused by a single fracture with a fracture specific stiffness of $5\text{x}10^{12}$ Pa/m.

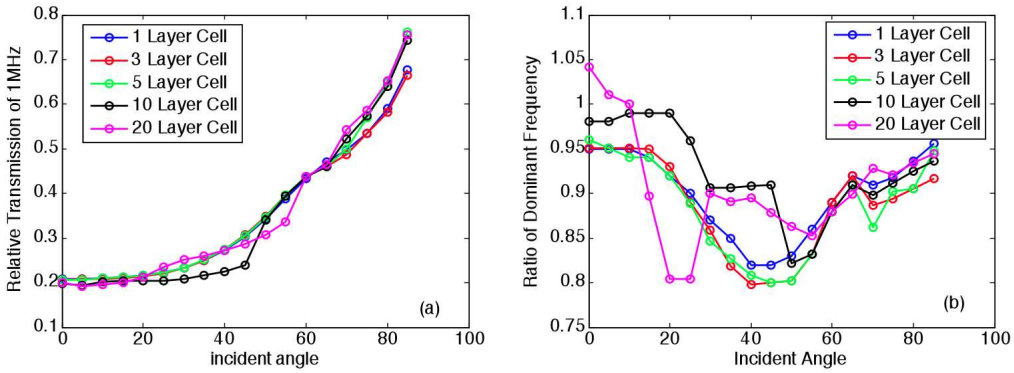

FIG. 10. *(left) Relative wave transmission for the 1MHz frequency component as a function of incident angle; (right) Ratio of the dominant frequency as a function of incident angle.*

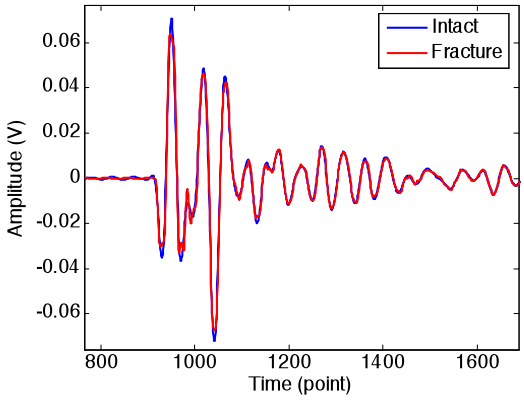

FIG. 11. *Wave propagated through an intact layered medium (red line), and a fractured layered medium for fracture specific stiffness Pa/m (blue line).*

4.2.3. Effect of fracture specific stiffness. Fracture specific stiffness varies among fractures in nature (Pyrak-Nolte et al., 1987; Pyrak-Nolte et al., 1990a; Pyrak-Nolte et al., 1996; Pyrak-Nolte & Morris, 2000; Worthington & Lubbe, 2006; Lubbe et al., 2007; Worthington, 2007). We also examined the effect of fracture specific stiffness on wave propagation through a fractured- layered medium for fracture specific stiffness of $5x10^9$ Pa/m, $5x10^{10}$ Pa/m, $5x10^{11}$ Pa/m, $5x10^{12}$ Pa/m, $5x10^{13}$ Pa/m, and $5x10^{14}$ Pa/m. In this preliminary study, the number of layered cells was 20 for a normally incident wave. When the fracture specific stiffness is $5x10^{14}$ Pa/mm or greater, the fractured layered medium transmits the signal as well as the non-fractured layered medium (Figure 11). A fracture is present but it cannot be detected at the frequencies used in these simulations ($\sim$ 0.01 MHz to 2 MHz). The fracture would be detected if higher frequency components were used in the simulations.

We have begun a parameter study to try to simulate the behavior observed in the experiments on sample AC1 and AC7. For the source signal, we used a compressional wave that was propagated through an Aluminum standard from source-receiver pair 2P-4P (Figure 2) at an incident angle of 57. The number of layered cells was 10. As observed in Figure 12, significant multiples were not generated as seen in the results from sample AC7 nor did we observe an increase as was observed in sample AC1.

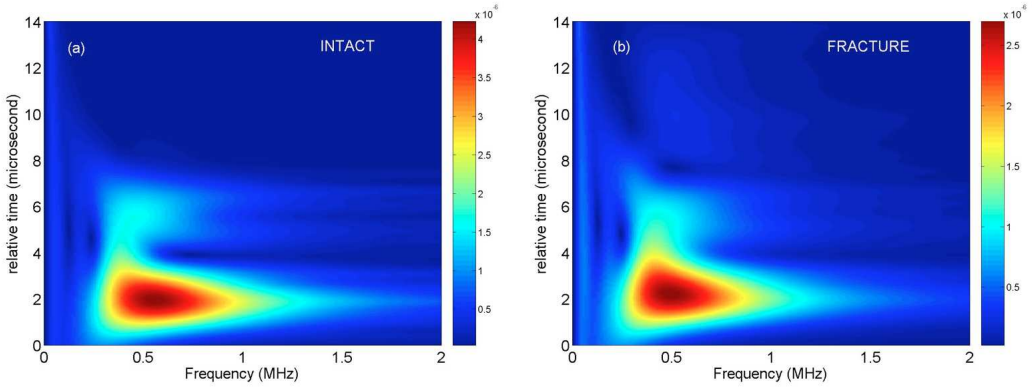

FIG. 12. *Wavelet transforms for signals propagated through 10 layered cells at an incident angle of 57° for (a) a layered medium and (b) a fractured layered medium.*

5. Conclusion. In the experimental data, we observed that the presence of a single fracture in a layered medium affects internal multiple reflections (constructive and destructive interference) that resulted in a higher dominant frequency for the fractured sample than the intact sample. From our initial theoretical study, we have not been able to reproduce the results we observed in the laboratory. However, we have not fully explored the parameter space of the theoretical model, namely varying the impedances of the layers, altering the unit layered cell, the order of the layers within the cell, thickness of the layer, etc. In addition, the theory must include the fracture orientations that are not parallel to the layering to improve the comparison to the experimental conditions where the fracture is oriented at 57° to the layers. Our goal is to fully understand the effects of a layered medium on the interpretation of fracture specific stiffness.

6. Acknowledgments. The authors wish to acknowledge support of this work by the Geosciences Research Program, Office of Basic Energy Sciences US Department of Energy (DEFG02-97ER14785 08) and by ExxonMobil Upstream Research Company

7. References.

1. Aki, K. and P. G. Richards, Quantitative Seismology, Theory and Methods, W. H. Freeman and Company, 1980.
2. Crampin, S., A review of wave motion in anisotropic cracked elastic media, Wave Motion 2, 1981, 343-391.
3. Jaeger, J.C. and N.G.W. Cook, Fundamentals of Rock Mechanics, 3rd Edition, Chapman Hall, London, 1979.
4. Li, W., Petrovitch, C., and L. J. Pyrak-Nolte, The effect of fabric-controlled layering on compressional and shear wave propagation in carbonate rock, Internation Journal of the JCRM, Japanese Committee for Rock Mechanics, Special Issue on Geophysics, Volume 4, Number 2, November 2009, pp 79-85.
5. Lubbe, R., Sothcott, J., Worthington, M. H. and C. McCann, Laboratory estimates of normal and shear fracture compliance, Geophysical Prospecting, v. 56, issue 2, 239-247, 2008.
6. Mal, A. K., Wave propagation in layered composite laminates under periodic surface loads, Wave Motion, v. 10, issue 3, 1988, 257-266.
7. ODoherty, R. F., N. A. Anstey, Reflections on Amplitudes. Geophysical Prospecting, 1971. 19: p. 430-458.
8. Petrashen, G. I., Propagation of Seismic Wave Fields in Layered Media, Journal of Mathematical Sciences, v.116, no. 2, 2003.

9. Pyrak-Nolte, L.J., Myer, L.R., Cook, N.G.W., and P.A. Witherspoon, Hydraulic and Mechanical Properties of Natural Fractures in Low Permeability Rock, 1987, Proceedings of the Sixth International Congress on Rock Mechanics, eds. G.
10. Herget & S. Vongpaisal, Montreal, Canada, August 1987, Pubs. A.A. Balkema (Rotterdam), pp.225-231.
11. Pyrak-Nolte, L. J., Myer, L. R. and N.G.W. Cook, 1990, Transmission of Seismic Waves across Single Natural Fractures, Journal of Geophysical Research, vol. 95, no. B6, pages 8617-8638, June 10, 1990).
12. Pyrak-Nolte, L. J., Mullenbach, B. L., and S. Roy, Interface waves along fractures, Journal of Applied Geophysics , 35, 79-87, 1996
13. Pyrak-Nolte, L. J. and J. P. Morris, Single fractures under normal stress: The relation between fracture specific stiffness and fluid flow, International Journal of Rock Mechanics Mining Science & Geomechanics Abstracts, vol 37, p245-262, 2000.
14. Worthington, M. H. and R. Lubbe, The scaling of fracture compliance, Geological Society, London, Special Publication, v. 270, 73-82, 2007.
15. Worthington, M. H., The compliance of macrofractures, The Leading Edge, v. 26, no. 9, 1118-1122, September 2007.